

# The role of excitons and trions on electron spin polarization in quantum wells.

P. Aceituno\* and A. Hernández-Cabrera†

*Dpto. Física Básica. Universidad de La Laguna. La Laguna. 38206-Tenerife. Spain*

(Dated: December 6, 2018)

We have studied the time evolution of the electron spin polarization under continuous photoexcitation in remotely  $n$ -doped semiconductor quantum wells. The doped region allows us to get the necessary excess of free electrons to form trions. We have considered electron resonant photoexcitation at free, exciton and trion electron energy levels. Also, we have studied the relative effect of photoexcitation energy density and doping concentration. In order to obtain the two-dimensional density evolution of the different species, we have performed dynamic calculations through the matrix density formalism. Our results indicate that photoexcitation of free electron level leads to a higher spin polarization. Also, we have found that increasing the photoexcitation energy or diminishing the doping enhances spin polarization.

PACS numbers: 73.20.Mf, 73.50.Gr, 73.40.Gk

## I. INTRODUCTION

In semiconductor heterostructures, and in an environment with an excess of electrons or holes, not only neutral excitons ( $X$ ) can be found but also negative or positively charged excitons, respectively. This happens because, under certain circumstances, excitons capture an extra charge to form the so called trions or charged excitons. Thus, trions represent bound states of three particles: two electrons and a hole in the case of negatively charged excitons ( $X^-$ ), and two holes and one electron in the case of positively charged excitons ( $X^+$ ). Bound complexes of three particles have a binding energy which is large enough to make them observable. The most broadly used experimental technique to investigate trions is the time-resolved photoluminescence<sup>1-3</sup>. Recently, generation and recombination processes of excitons and trions have been analyzed using this technique<sup>4,5</sup>. Photoluminescence has also been used to investigate two-dimensional electron gas (2DEG) in magnetic fields<sup>6</sup>.

A trion can be formed by photoexcitation together with selectively doping to get the charge excess or, alternatively, only by injection or diffusion of electrons and holes. There are three ways to form trions in photoexcitation. Directly,

by the resonant excitation of trion electron level and the trapping of a second electron (or hole) . Indirectly, either by the excitation of an electron-hole pair, followed by the formation of an exciton, or by resonant excitation of a neutral exciton. In the latter two cases the exciton, after its formation, is attached to an existing free electron (or hole). The dynamics of the three processes are different<sup>7</sup>. The other method involves the injection of electrons and holes by doping regions close to the structure. Injection has the advantage of avoiding the interaction between the electromagnetic field associated with the photoexcitation and the excited electrons<sup>8,9</sup>.

Spintronics has newly aroused great interest in the scientific community due to its promising future for creating circuits faster and more efficient than that existing in semiconductor devices. To paraphrase Awschalom et al., the reason is that the energy needed to generate and transport electron spins is much less than that necessary to create charge electron currents. In practice, the main obstacle that faces spintronics is to produce polarized spin currents without loss of polarization during the process<sup>10</sup>.

One of the main properties of trions is precisely their influence on the polarization and duration of the electron spin in semiconductor quantum wells (QWs) and, thus, in spintronics<sup>11,12</sup>. At zero magnetic field the ground state of the trion is a singlet, that is, the two electrons (or holes) have opposite spins. The trion triplet state, in which the two electrons (holes) have the same spin direction, is not bound at zero magnetic field. Triplet state only becomes bound under finite magnetic fields. As mentioned above, the trion state consists of two charges belonging to the most abundant group and the remaining charge belonging to the minority of the total carrier concentration. Both types of carriers may have two directions of angular momentum (in a typical quantum well,  $\pm 3/2$  for heavy holes and  $\pm 1/2$  for electrons). In the singlet state the total angular momentum coincides with the angular momentum of the minority carriers, either holes in  $X^-$  or electrons in  $X^+$ . The triplet state is observed only in high magnetic fields or when the Zeeman splitting is greater than the energy separation between singlet and triplet states<sup>6,13-16</sup>. Since its simplicity, the singlet state is particularly suitable for the study of the spin dynamics.

In the last years several works have considered photoexcitation and spin polarization in different semiconductor structures and under different resonance conditions. Dynamic studies of spin polarization, including exciton and trion contributions, can be found in the literature<sup>17-20</sup>. Some authors have reported the resonant photoexcitation at the exciton or trion electron levels is the suitable way to get the spin coherence during a reasonably long time to be used in spintronic devices, without the help of applied magnetic fields or tunneling from magnetic impurities<sup>21,22</sup>. Others

say it is better resonant photoexcitation of free electron level<sup>23</sup>. However, still is open the question about the relation between resonance and efficiency. To be precise, what happen if the energy of photoexcitation resonates with the free electron level, the exciton level, or the trion level. If the excitation energy is in resonance with one level or another, the situation will be different. In this work we will compare the three choices just mentioned and show that the resonant free electron excitation leads to a higher spin polarization, by means of the intermediate contribution of excitons and trions. We will consider a long duration pulse to study its effect on the spin polarization.

Suppose we have a quantum well doped in the left barrier, as Fig. 1 shows. Applying a suitable low electric field we can vary the relative position of the Fermi level with respect to the ground level of the conduction well, controlling the electron density injected by tunneling into the well. When we photoexcite free electrons coherently, if the excitation pulse is long enough, free electrons will form excitons through the Coulomb interaction with remaining holes. In addition, as the material is slightly doped with donors, the appearance of negative trions is an immediate consequence. Note that, in quantum wells, the strong dipole-dipole repulsion between excitons prevents the formation of biexcitons. Thus, contributions from these neutral species can be overlooked<sup>24</sup>. Thus, we deal with three different electronic states (free, excitonic, and trionic electron) which will occupy different energy levels.

While free electrons from doping have their spins randomly oriented, it does not happen the same for photoexcited electrons if illuminating with polarized light: photoexcited species have a dominant spin orientation controlled by the polarization of the photon. For example, applying a circularly polarized light  $\sigma^+$ , holes are spin up orientated whilst electrons are spin down<sup>25</sup>. Because of this preferred orientation one can achieve a net electron spin polarization for practical purposes. The aim of this paper is the theoretical analysis of the temporal evolution of the spin polarization for electrons when semiconductor QW is doped with different concentrations and photoexcited at different laser frequencies, corresponding to free electron, exciton or trion resonance. Besides, we will analyze the duration of the spin polarization depending on the relationship between doping and photoexcitation energy density. We will consider all the possible processes of generation and annihilation of excitons, trions and free electrons. In general, we will not consider in detail the specific physical processes that lead to different relaxation times (Dyakonov-Perel, Elliott-Yafet, Bir-Aronov-Pikus mechanisms, and so on). These processes have been carefully analyzed elsewhere<sup>11,12</sup>. Therefore, we chose empirical relaxation times for the simplest case, where there are no external fields (except a very low electric field necessary to inject the free electrons into the QW), inhomogeneities in the interfaces, interaction with the nuclear

spin, etc.

We will show that, although the presence of trions is essential to preserve a reasonable spin polarization, photoexcitation of electrons at trion level is not necessary. We use the matrix density formalism, considering the different generation, recombination and annihilation rates for different types of binding energy and spin polarization<sup>26</sup>. The effect of the interband optical pulse is included through the interband generation function.

We will first consider the Bloch equations for the general dynamics of the spin polarization for the different species. Then, we will consider the three cases mentioned before, corresponding to the photoexcitation energy in resonance with free electron, exciton or trion level.

## II. GENERAL DYNAMICS

We assume an ultrafast  $\delta(t)$  injection of electrons from the doped region into the QW to simplify calculations, when the electronic level lays under the Fermi level. This assumption can be removed if selective doping is deemed. We consider the excitation laser pulse by the function

$$w(t) = \frac{1 + \cosh(\tau_p/2\tau_f)}{[\cosh((t - t_0)/\tau_f) + \cosh(\tau_p/2\tau_f)]}, \quad (1)$$

where  $\tau_p$  is the pulse duration and  $10\tau_f$  is the front pulse duration. Thus, for  $\tau_f = 0$  ps we have a square pulse and, for  $\tau_f > \tau_p$ , the pulse in a gaussian-like one<sup>26</sup>. We simulate a continuous regime excitation by a very long pulse with  $\tau_p = 2000$  ps and  $\tau_f = 10$  ps. To consider a pulse starting at  $t = 0$  ps, we have introduced the shift  $t_0 = (\tau_p + 10\tau_f)/2$ .

We first consider the general quantum kinetic equation for the density matrix operator  $\hat{\eta}(t)$ , and for electrons placed in an electric field with frequency  $\omega$ ,  $\mathbf{E}(t) \exp(-i\omega t) + c.c. = \mathbf{E}w(t) \exp(-i\omega t) + c.c.$ ,

$$\frac{\partial \hat{\eta}(t)}{\partial t} + \frac{i}{\hbar} [\hat{H}, \hat{\eta}(t)] = \frac{1}{i\hbar} \left[ \left( \widehat{\delta H}_t \exp(-i\omega t) + H.c. \right), \hat{\eta}(t) \right]. \quad (2)$$

Here  $\hat{H}$  is the QW one-particle many-band Hamiltonian we have described elsewhere<sup>27</sup>. When electrons are excited by the transverse electric field associated to the laser pulse,  $E_{\perp} w(t) \exp(-i\omega t) + c.c.$ , the perturbation operator  $\widehat{\delta H}_t$ , which describes interband transition, can be written as<sup>28</sup>

$$\widehat{\delta H}_t = (ie/\omega) E_{\perp} \hat{v}_{\perp} w(t), \quad (3)$$

where  $\hat{v}_{\perp}$  is the transverse velocity operator. If we project on the conduction band states we find the kinetic equation

for the one-electron density matrix  $\widehat{\rho}(t)$

$$\frac{\partial \widehat{\rho}(t)}{\partial t} + \frac{i}{\hbar} [\widehat{H}, \widehat{\rho}(t)] = \widehat{G}(t) + \widehat{J}(\widehat{\rho}|t), \quad (4)$$

where  $\widehat{J}(\widehat{\rho}|t)$  is the collision integral and the generation rate is given by

$$\widehat{G}(t) = \frac{1}{\hbar^2} \int_{-\infty}^0 d\tau e^{\lambda\tau - i\omega\tau} \left[ e^{i\widehat{H}\tau/\hbar} [\widehat{\delta H}_{t+\tau}, \widehat{\rho}_{eq}] e^{i\widehat{H}\tau/\hbar}, \widehat{\delta H}_t^+ \right] + H.c. \quad (5)$$

with the phenomenological constant  $\lambda \rightarrow +0$ . This constant is the finite relaxation rate. Here  $\widehat{\rho}_{eq}$  is the equilibrium density matrix when the second-order contributions to the response are taken into account.

Taking the basis  $\widehat{H}|\phi_\alpha\rangle = \varepsilon_\alpha|\phi_\alpha\rangle$ , we can rewrite Eq. (3) as a system of kinetic equations for  $f_{\alpha\beta}(t) = \langle \phi_\alpha | \widehat{\rho}(t) | \phi_\beta \rangle$ , where we neglect non-diagonal terms if  $(\varepsilon_\alpha - \varepsilon_\beta)/\hbar$  are larger than the collision relaxation and generation rates. Thus, for the diagonal terms,

$$\frac{\partial f_{\alpha\alpha}(t)}{\partial t} = G_\alpha(t) + J(f_{\alpha\alpha}|t), \quad (6)$$

where  $G_\alpha(t)$  is the photogeneration rate for the  $\alpha$  state, and  $J(f_{\alpha\alpha}|t)$  is the collision integral rate. Using the dipole approximation and the basis  $|\phi_\alpha\rangle = |n_\alpha\rangle$ , with  $\alpha = v$  (valence),  $c$  (conduction), we get

$$\begin{aligned} \frac{dn_c(t)}{dt} &= G(t) + \left( \frac{\partial n_c}{\partial t} \right)_{sc}, \\ \frac{dn_v(t)}{dt} &= -G(t) + \left( \frac{\partial n_v}{\partial t} \right)_{sc}, \end{aligned} \quad (7)$$

where  $n_{v,c}(t)$  are the electron densities in the valence and conduction bands. For the case in which there is only photoexcitation, terms  $\left( \frac{\partial n_c}{\partial t} \right)_{sc} = -\left( \frac{\partial n_v}{\partial t} \right)_{sc}$  correspond to the collision-induced relaxation of population in the conduction and valence bands. If we define the detuning energy as  $\Delta = \hbar\omega - (\varepsilon_c - \varepsilon_v)$ , the interband generation rate can be expressed through

$$G(t) = 2 \left( \frac{eE_\perp v_{cv}}{\hbar\omega} \right)^2 w(t) \text{Re} \left[ \int_{-\infty}^0 d\tau w(t+\tau) \sin \left( \frac{\Delta\tau}{\hbar} \right) \right], \quad (8)$$

and  $v_{cv}$  is the interband velocity. We will use the reduced generation function  $g(t) = G(t)/N_{ph}$  where

$$N_{ph} = 2\pi\rho_{2D} [eE_\perp v_{cv} \langle \phi_c(z_e) | \phi_v(z_h) \rangle / \omega]^2 \tau_p / \hbar \quad (9)$$

is the characteristic density of photoexcited charges (for  $\Delta = 0$  meV and  $\tau_p = 2000$  ps, an excitation energy density of  $1 \text{ nJ cm}^{-2}$  corresponds to a characteristic density of  $10^{10} \text{ cm}^{-2}$  in our structure). It is important to point out that

for such a long pulse, a detuning energy of  $\Delta = 0.01$  meV is enough to reach the maximum of the generation function  $g(t)$  (Fig. 2)<sup>26</sup>. Thus, we will use this value in calculations.

Since we will consider three photoexcitation cases, we will take into account three possibilities:  $\hbar\omega_i = (\varepsilon_c - \varepsilon_{b,i} - \varepsilon_v) + \Delta$  corresponding to the laser energies  $\hbar\omega_i$  ( $i = e, exc, tr$ ) for free, excitonic and trionic electrons, which resonate with their respective levels  $\varepsilon_c$ ,  $\varepsilon_c - \varepsilon_{b,exc}$  and  $\varepsilon_c - \varepsilon_{b,tr}$ , where  $\varepsilon_{b,i}$  is the exciton or trion binding energy (obviously  $\varepsilon_{b,e} = 0$ ). Thus, we will have three generation functions  $g_i(t)$  depending on the level resonance.

In the previous presentation of the density matrix we have not consider the spin of the particles. Let us do. To study the time evolution of the electron spin polarization, we first perform expressions for the temporal evolution of free electron, hole, exciton, and negative trion densities, paying attention to their spin orientation. We will consider the three possible generation functions as well as all other processes of generation and annihilation of these species. We will also consider the spin flip of electrons and holes. Then, we will particularize these expressions to the three cases under study.

Initially, free electrons are injected into the QW, through the left barrier, quasi-instantaneously and without any spin polarization. The probability of spin  $+1/2$  ( $e \uparrow$ ) or  $-1/2$  ( $e \downarrow$ ) is the same. Applying a circularly polarized light  $\sigma^+$  with energy  $\hbar\omega_e = (\varepsilon_c - \varepsilon_v) + \Delta$ , electron-hole pairs are generated with the peculiarity that the hole angular momentum is  $+3/2$  ( $h \uparrow$ ) and that of the electron is  $-1/2$  ( $e \downarrow$ )<sup>11</sup>. Since the spin flip time of the holes is very small in comparison with the duration times of the remaining involved events, holes with angular momentum  $-3/2$  ( $h \downarrow$ ) almost immediately appear. As the time of spin flip of electrons is several orders of magnitude greatest than the rest of processes, it will only affect to the behavior of the system at very long times. Nevertheless we will include it in our calculations.

The Coulomb interaction between electrons (injected or photoexcited) and holes creates the exciton because the binding energy reduces the energy of the system, leading to a more stable state. Initially all the holes, which have angular momentum  $+3/2$  ( $h \uparrow$ ), will join to electrons  $-1/2$  ( $e \downarrow$ ) to give rise to excitonic bosons with angular momentum  $+1$  ( $exc \uparrow\downarrow$ ). Almost simultaneously, given the fast spin flip of the photoexcited holes, holes  $-3/2$  ( $h \downarrow$ ) and electrons  $+1/2$  ( $e \uparrow$ ) give rise to excitons with angular momentum  $-1$  ( $exc \downarrow\uparrow$ ). We consider that nonoptical active excitons with the same orientation of electron and hole spins cannot be photoexcited or recombined. Inclusion of these cases in the Bloch equations would lead to nonsense results.

The interaction of excitons with the remaining low-density electron gas leads to the formation of trions. Excitons ( $exc \uparrow\downarrow$ ), in which the electron has spin  $-1/2$  ( $e \downarrow$ ), together with free electrons of spin  $+1/2$  ( $e \uparrow$ ), form trions (and conversely for the other orientation). The angular momentum of these trions ( $tr \uparrow$ ,  $tr \downarrow$ ) coincides with the corresponding angular momentum of holes, because the electron spins are compensated each other. Another possibility is the direct formation of trions by the Coulomb interaction between electrons and holes without intermediary pseudoparticles. The choices for angular momentum of these trions are the same already mentioned.

When the circularly polarized light  $\sigma^+$  has energy  $\hbar\omega_{exc} = (\varepsilon_c - \varepsilon_{b,exc} - \varepsilon_v) + \Delta$ , excitons are directly generated, with the same angular momentum presented before,  $+1$  ( $exc \uparrow\downarrow$ ) with hole angular momentum of  $+3/2$  ( $h \uparrow$ ) and electron angular momentum of  $-1/2$  ( $e \downarrow$ ). As in the former example, these excitons can produce trions  $+3/2$  ( $tr \uparrow$ ) through their interaction with free electrons  $+1/2$  ( $e \uparrow$ ).

And, in the last case, when the energy of the polarized light resonates with the trion level,  $\hbar\omega_{tr} = (\varepsilon_c - \varepsilon_{b,tr} - \varepsilon_v) + \Delta$ , the  $+3/2$  ( $tr \uparrow$ ) trions are generated by the capture of free electrons  $+1/2$  ( $e \uparrow$ ).

The above mentioned mechanisms take some time expressed through the generation rates  $F_{exc}$ ,  $F_{tr}$ , and  $F_{tr2}$ . The inverse of the mean time needed for exciton formation is  $F_{exc}$ , and  $F_{tr}$  is the trion formation rate via three-particle processes: two free electrons and a hole for negative trion. And  $F_{tr2}$  is the trion formation rate through two-particle interaction: an exciton plus a free electron.

About the disappearance of the mentioned species, we will consider three mechanisms. First, the direct recombination of a free electron with a hole. Second, the recombination of an electron and a hole within an exciton, as well as the dissociation of the exciton resulting in an electron and a hole. And third, the recombination of an electron with a hole within a trion leaving free the other electron, together with the dissociation of a trion in two or three particles. In the following expressions,  $R_e$  is the radiative recombination coefficient of free carriers,  $R_{exc}$  and  $R_{tr}$  are the inverse of the intrinsic exciton and trion lifetimes, respectively. Dissociation rates for both excitons and trions are so small that neglecting their effect do not change results (Appendix A).

Moreover, electrons lose their free condition when producing excitons and trions. So the generation rates  $F_{exc}$ ,  $F_{tr}$ , and  $F_{tr2}$  contribute also as three additional mechanisms for free electron extinction. Further, trion annihilation gives rise to free electrons because the recombination of one electron with the hole leaves an extra free electron. Thus, we have another generation term for free electrons at a rate  $R_{tr}$ . We also define  $S_e$  and  $S_h$  as the spin flip rate for

electrons and holes, respectively.

By writing densities of free electrons, holes, excitons, and negative trions in units of  $N_{ph}$  [ $n_e(t)$ ,  $n_h(t)$ ,  $n_{exc}(t)$ , and  $n_{tr}(t)$ , respectively] we project over the two spin states. We will consider free electrons from doping included in the initial boundary conditions,  $n_e(t=0) = N_D/N_{ph}$  which, projected onto the spin states reads  $n_{e\uparrow}(t=0) = n_{e\downarrow}(t=0) = N_D/2N_{ph}$ , where  $N_D$  is the total density of injected electrons. The remaining densities are equal to zero before switching the pulse on.

For free electrons we have

$$\begin{aligned} \frac{d}{dt}n_{e\uparrow}(t) &= -F_{exc}n_{e\uparrow}(t)n_{h\downarrow}(t) - F_{tr2}n_{e\uparrow}(t)n_{exc\downarrow\uparrow}(t) - F_{tr}n_{e\uparrow}(t)n_{e\downarrow}(t) [n_{h\uparrow}(t) + n_{h\downarrow}(t)] \\ &\quad + R_{tr}n_{tr\uparrow}(t) - R_en_{e\uparrow}(t)n_{h\downarrow}(t) + S_e [n_{e\downarrow}(t) - n_{e\uparrow}(t)] - g_{tr}(t)n_{e\uparrow}(t), \\ \frac{d}{dt}n_{e\downarrow}(t) &= g_e(t) - F_{exc}n_{e\downarrow}(t)n_{h\uparrow}(t) - F_{tr2}n_{e\downarrow}(t)n_{exc\uparrow\downarrow}(t) - F_{tr}n_{e\downarrow}(t)n_{e\uparrow}(t) [n_{h\uparrow}(t) + n_{h\downarrow}(t)] \\ &\quad + R_{tr}n_{tr\downarrow}(t) - R_en_{e\downarrow}(t)n_{h\uparrow}(t) + S_e [n_{e\uparrow}(t) - n_{e\downarrow}(t)]. \end{aligned} \quad (10)$$

In a similar way, excitonic electrons appear at a rate  $F_{exc}$  and disappear due to recombination and trion generation at rates  $R_{exc}$  and  $F_{tr2}$ , respectively. Thus, for excitonic electrons,

$$\begin{aligned} \frac{d}{dt}n_{exc\downarrow\uparrow}(t) &= g_{exc}(t) + F_{exc}n_{h\uparrow}(t)n_{e\downarrow}(t) - R_{exc}n_{exc\downarrow\uparrow}(t) - F_{tr2}n_{exc\downarrow\uparrow}(t)n_{e\uparrow}(t), \\ \frac{d}{dt}n_{exc\uparrow\downarrow}(t) &= F_{exc}n_{h\downarrow}(t)n_{e\uparrow}(t) - R_{exc}n_{exc\uparrow\downarrow}(t) - F_{tr2}n_{exc\uparrow\downarrow}(t)n_{e\downarrow}(t) \end{aligned} \quad (11)$$

and, for up and down trion electrons,

$$\begin{aligned} \frac{d}{dt}n_{tr\uparrow}(t) &= g_{tr}(t)n_{e\uparrow}(t) + F_{tr2}n_{e\uparrow}(t)n_{exc\downarrow\uparrow}(t) + F_{tr}n_{e\uparrow}(t)n_{e\downarrow}(t)n_{h\uparrow}(t) - R_{tr}n_{tr\uparrow}(t) + S_h [n_{tr\downarrow}(t) - n_{tr\uparrow}(t)], \\ \frac{d}{dt}n_{tr\downarrow}(t) &= F_{tr2}n_{exc\uparrow\downarrow}(t)n_{h\downarrow}(t) + F_{tr}n_{e\downarrow}(t)n_{e\uparrow}(t)n_{h\downarrow}(t) - R_{tr}n_{tr\downarrow}(t) + S_h [n_{tr\uparrow}(t) - n_{tr\downarrow}(t)]. \end{aligned} \quad (12)$$

Lastly, for the hole density we can write

$$\begin{aligned} \frac{d}{dt}n_{h\uparrow}(t) &= g_e(t) - F_{ex}n_{h\uparrow}(t)n_{e\downarrow}(t) - F_{tr}n_{e\uparrow}(t)n_{e\downarrow}(t)n_{h\uparrow}(t) - R_en_{h\uparrow}(t)n_{e\downarrow}(t) + S_h [n_{h\downarrow}(t) - n_{h\uparrow}(t)], \\ \frac{d}{dt}n_{h\downarrow}(t) &= -F_{ex}n_{h\downarrow}(t)n_{e\uparrow}(t) - F_{tr}n_{e\uparrow}(t)n_{e\downarrow}(t)n_{h\downarrow}(t) - R_en_{h\downarrow}(t)n_{e\uparrow}(t) + S_h [n_{h\uparrow}(t) - n_{h\downarrow}(t)]. \end{aligned} \quad (13)$$

To analyze particle densities we numerically perform the coupled system (10-13) using the Runge-Kutta method. We only consider cases in which the excess of free electron density is of about  $10^{10}cm^{-2}$ . For densities higher than these, the effect of the electron-electron Coulomb interaction becomes more remarkable because of the space-charge



potential energy created by the spatial distribution of electrons and holes. This space-charge potential is repulsive for holes and attractive for electrons. At low densities, electron-hole attraction dominates over electron-electron and hole-hole repulsion. When the carrier density increases, the repulsive part of the Hartree-Fock potential energy increases as well. Beyond a certain initial density ( $n_e(0) \gtrsim 10^{11} \text{ cm}^{-2}$ ) of free electrons, the repulsion equals the attractive potential. For higher densities the Coulomb interaction of the second electron with the hole in the trion is canceled, resulting in trion extinction, which creates excitons and free electrons. If the free electron density increases further, the binding energy of excitons tends to zero and these species also disappear. These densities mainly affect the dynamics of the energy level shift of electrons<sup>3,26,27</sup>.

To study the influence of the relation between doping and photoexcitation energy density on the evolution of the different particle densities  $n_i(t)$  (where  $i = e \uparrow, e \downarrow, exc \uparrow\downarrow, exc \downarrow\uparrow, tr \uparrow, tr \downarrow, h \uparrow, h \downarrow$ ), we consider in calculations two photoexcitation characteristic densities and two doping concentrations. To standardize equations, we take a referral density  $N_0$  as normalization constant for  $n_i(t)$  at any case. Then, in a first case (A) we consider this referral density equal to the photoexcited electron and the injected electron densities ( $N_0 = N_{ph} = N_D$ ). This situation is reflected in the initial boundary conditions stating  $n_{e\uparrow}(t=0) = n_{e\downarrow}(t=0) = 0.5$  in  $N_0$  units. In a second case (B) we keep the same doping ( $N_D = N_0$ ) and use a  $N_{ph}$  ten times bigger than the used before ( $N_{ph} = 10N_0$ ), which corresponds to an excitation energy density ten times higher, approximately. The initial boundary conditions do not change. In a last case (C) we return to the first photoexcited electron density ( $N_{ph} = N_0$ ) but reduce the injected electron density ( $N_D = N_0/10$ ). This means that doping concentration is ten times lower in referral density units. So the initial boundary conditions will be  $n_{e\uparrow}(t=0) = n_{e\downarrow}(t=0) = 0.05$ .

There is a large and sparse number of values for the coefficients involved in these equations (10-13), depending on the characteristics of the samples, theories, or experimental conditions. These can be found in the related literature, where there are many information available. Phenomenological and theoretical data for electron spin relaxation and for GaAs-GaAlAs QWs are included in many papers<sup>29-33</sup>. Also, data for hole spin flip times can be found in the literature<sup>34-36</sup>. An extensive analysis of the formation, recombination and dissociation coefficients can be found in the papers of Esser et al.<sup>1</sup> and Portella-Oberli et al.<sup>4,37</sup>. Following these last references and considering the mass action law (Saha-Eggert relations), we have evaluated the corresponding values for our structure (Appendix A). Table I shows numerical values of the coefficients used in this work. We have found the process of exciton generation is

$R_e$	$F_{exc}$	$R_{exc}$	$F_{tr2}$	$F_{tr}$	$R_{tr}$	$S_e$	$S_h$
$10^{-4}$	$2 \times 10^{-2}$	$2.5 \times 10^{-3}$	$6 \times 10^{-3}$	$2 \times 10^{-3}$	$4.5 \times 10^{-3}$	$10^{-4}$	$2.6 \times 10^{-2}$

TABLE I: Characteristic generation and relaxation coefficients in  $\text{ps}^{-1}$ , for low temperature (5 K).

much faster than the formation of trions and the annihilation of both excitons and trions. Further, trion generation by means of excitons ( $F_{tr2}$ ) is a mechanism faster than trion formation from three elements ( $F_{tr}$ ), as expected. On the other hand, trion recombination is faster than this last formation mechanism.

Next, we calculate the electron spin relative polarization defined as the difference between spin down and spin up free electron concentrations divided by their sum,  $p(t) = (n_{e\downarrow}(t) - n_{e\uparrow}(t)) / (n_{e\downarrow}(t) + n_{e\uparrow}(t))$ .

Finally, we compare temporal evolution of normalized densities  $n_i(t)$  and electron spin relative polarization  $p(t)$ , for the three above mentioned cases of photoexcitation and doping (A, B and C), when resonant photoexcited level corresponds to free, exciton or trion electron energy level (cases 1, 2 and 3, respectively).

### III. RESULTS AND DISCUSSION

#### A. Case 1. Resonant photoexcitation of free electron.

The spin polarization of the free electron gas takes place essentially by the proper photoexcitation, because  $\sigma^+$  polarized light generates spin down but not spin up electrons.

First, we will analyze the role that play the different processes on the net polarization for the case (A). In the hypothetical case in which only doping and photoexcitation coexist, without any other process, spin up electron concentration would remain constant, whereas spin down electron concentration linearly increases while the pulse is present (Fig. 3a), which would produce certain polarization ‘per se’. These spin down and spin up electron concentrations will be slightly affected by the inclusion of the free electron-hole recombination along with the rapid flip of the hole spin (Fig. 3b). They will change most appreciably for a realistic case, when all the different processes of bimolecular creation and destruction of excitons (Fig. 3c) or excitons and trions (Fig. 3d) are included.

The holes generated during the photoexcitation have spin up but, since the hole flipping time is very short, it is possible to consider a similar number of holes with spin up or down. However, due to the very slow flip of the electron spin, the density of spin down electrons ( $e\downarrow$ ) is greater because of the light polarization. As a consequence

of its higher density, free electron recombination is greater for these spin down electrons. This could be explained by considering the situation where spin up free holes ( $h \uparrow$ ) can find easier this kind of free electrons ( $e \downarrow$ ) to recombine with (Fig. 3b).

For the same reason, the disappearance of up and down electrons during the exciton formation process is not balanced: spin down electrons form more excitons ( $exc \uparrow\downarrow$ ) than the others. Thus, a clear decrease of spin down electron ( $e \downarrow$ ) density, bigger than the corresponding for spin up electrons, can be observed by comparing Fig. 3c with Fig. 3b. On the other hand, the recombination of excitons is independent of the relative concentration for any spin orientation because each electron in exciton is associated to a hole and its recombination does not depend on others. Moreover, exciton recombination does not influence both spin electron densities.

Since both electrons in trion have different spin orientation, three particle trion formation leads to a balanced up and down electron quenching. When the formation of trions arises from excitons, there are two possibilities: excitons ( $exc \uparrow\downarrow$ ) together with spin up electrons ( $e \uparrow$ ) to give trions ( $tr \uparrow$ ) or excitons ( $exc \downarrow\uparrow$ ) with spin down electrons ( $e \downarrow$ ) to give trions ( $tr \downarrow$ ). As we mentioned above, there are a greater amount of these electrons ( $e \downarrow$ ) and of the former excitons ( $exc \uparrow\downarrow$ ), leading to a balanced formation of trions with both spin orientations. Thus, electrons with both spin orientation disappear at a similar rate. Moreover, as the spin of electrons in trion is compensated, the spin of the hole in trion is able to flip and so, we can find trions with spin up and down with almost the same probability. The same reasoning for exciton recombination applies to trions recombination. In this case, the recombination of the electron-hole pair in trion frees an electron, whose spin orientation is equiprobable due to the similar density of the two kind of trions. In order to show all these behaviors we have added Fig. 4, which corresponds to a magnified version of Fig. 3d, with the curves split for the different spin orientations for holes, excitons, and trions.

The resulting relative polarization  $p(t)$  will reflect all the changes above reported. In Fig. 5 we show the polarization calculated for each case included in Fig. 3. Thus, in the case depicted in Fig. 3a,  $n_{e\downarrow}(t)$  increases linearly along the pulse duration giving the largest difference of densities ( $n_{e\downarrow}(t) - n_{e\uparrow}(t)$ ). However, the relative polarization is not the best because also the total amount of electrons ( $n_{e\downarrow}(t) + n_{e\uparrow}(t)$ ) is the biggest. The inclusion of the free electron-hole recombination is not very noticeable in the concentrations behavior (Fig 3b) but it affects to the polarization leading to the lowest values. Polarization increases when the different processes of creation and annihilation of excitons are included (corresponding to Fig. 3c), because the total density of electrons with different spins is lower. And so, when

also creation and destruction of trions are considered (Fig 3d), the relative polarization reaches their greatest values.

The influence of the photoexcitation energy density and the doping on the different species normalized densities can be seen in Fig. 6, where we compare the three cases mentioned before: (A) with  $N_{ph} = N_D = N_0$ , (B) with  $N_{ph} = 10N_0$ ,  $N_D = N_0$ , and (C) with  $N_{ph} = N_0$ ,  $N_D = N_0/10$ . In the upper panel we represent case (A), which corresponds to case considered in the former Figs. 3d and 4. The middle panel displays case (B), where the same doping as in (A) but ten times bigger characteristic photoexcitation density leads to a considerable increase of excitons ( $exc \uparrow\downarrow$ ), whose density even exceeds that of the electrons ( $e \downarrow$ ). Now there is also a significant trion concentration. The lower panel shows the last case (C), where photoexcitation energy density goes back to the value of (A), but doping is ten times lower. Although the relation between  $N_{ph}$  and  $N_D$  recovers the previous case ( $N_{ph} = 10N_D$ ), the behavior of normalized densities  $n_i(t)$  is clearly different. In this case, the bigger influence of the photoexcitation leads to a big increase on the relative density of spin down electrons ( $e \downarrow$ ) and spin up holes ( $h \uparrow$ ). Now, the exciton ( $exc \uparrow\downarrow$ ) formation is not as faster as in (B) and a greater variation in densities of spin up and spin down electrons is obtained. As in (A), trion density is practically negligible.

Fig. 7 displays the resulting relative polarization for the three cases considered. One can see the clear improvement of the electron spin polarization when characteristic photoexcitation density exceeds doping density ( $N_{ph} = 10N_D$ , cases B and C). Moreover, relative polarization is better when increasing  $N_{ph}$  (B) than when diminishing  $N_D$  (C).

### B. Case 2. Resonant photoexcitation of excitons.

When excitons are photoexcited resonantly<sup>23</sup>, the only free electrons that exist are those from the doped region (this is only strictly true at low temperatures; if the temperature increases electrons and holes preferred free carriers position). Moreover, because of all the holes are bound in excitons, there are not free holes. Due to the circularly polarized light  $\sigma^+$ , photoexcited excitons are ( $exc \uparrow\downarrow$ ) and their only alternative to form trions is to join spin up free electrons ( $e \uparrow$ ) from the doping, leading initially to specific trions ( $tr \uparrow$ ). But, because of the fast spin flip of the hole in trion we will find, after several picoseconds, balanced densities for trions ( $tr \uparrow$ ) and ( $tr \downarrow$ ). Thus, the recombination of an electron-hole pair in these trions will leave spin up and spin down electrons with the same probability. In this case, since there are not free holes to bind with free electrons from doping, there is not the possibility of having

excitons ( $exc \downarrow\uparrow$ ); there will exist only photoexcited ( $exc \uparrow\downarrow$ ) ones.

Fig. 8 shows the density time evolution for the different species and for the same three cases of Fig. 6. As expected, resonance with free electron or exciton level leads to a faster increase of the relative density of spin down electrons ( $e \downarrow$ ) or excitons ( $exc \uparrow\downarrow$ ), respectively. The difference between the two kinds of resonant photoexcitation is more obvious in lower panels (B and C), when  $N_{ph} = 10N_D$ . By comparing upper panel (corresponding to case A) in both figures, a smaller difference between spin up and down free electron densities can be seen for this exciton resonance case. This is more evident as we go through cases B and C. Accordingly, this kind of resonant photoexcitation does not present any improvement for spin polarization. Fig. 9 depicts the relative electron spin polarization, showing a clear improvement when increasing the photoexcitation energy density (case B), as it occurred formerly (Fig. 7). However, for the other cases (A and C), spin polarization does not increase as much as when light resonated with free electrons.

### C. Case 3. Resonant photoexcitation of trions.

Finally, we analyze the case of resonant photoexcitation with the trion level. In this case, trions ( $tr \uparrow$ ) are directly generated by means of the capture of free electrons ( $e \uparrow$ ) and without exciton intervention<sup>38</sup>. As in the previous case, the unique free electrons we have are the injected ones, and there are not free holes. So, as there are not free holes to join injected free electrons, there is not the possibility of having excitons at all. We will find just photoexcited trions and free electrons. The circularly polarized light  $\sigma^+$  initially photoexcites specific trions ( $tr \uparrow$ ) and, due to the fast spin flip of the hole in trion, we will have balanced densities for trions ( $tr \uparrow$ ) and ( $tr \downarrow$ ), as in the exciton resonant case.

Fig. 10 presents the evolution of the normalized density for the three situations under study. Due to the balanced densities of the two orientations, trions ( $tr \uparrow$ ) and ( $tr \downarrow$ ), we have drawn the sum of both curves in only one. While in the first case (A) behavior is very similar to the former ones (Figs. 6 and 8), does not happen the same when  $N_{ph} = 10N_D$  (B and C). In case (B), with  $N_{ph} = 10N_0$ ,  $N_D = N_0$ , we can see a fast increase of the relative density of trions, as expected for the photoexcited species but it is clearly less than that shown in Figs. 6-8. The reason is that now, to generate trions, there must be free electrons available to be captured. Since the only electrons we have come from the injected from the doped region, this electron density determines the possible photoexcited trion

density. Also, because only up free electrons ( $e \uparrow$ ) are captured during photoexcitation, the density of these electrons drastically decreases. However, trion recombination leaves a compensated density of up and down free electrons.

For  $N_{ph} = N_0$ ,  $N_D = N_0/10$  (C), differences are more remarkable among this and the two other cases (Figs. 6 and 8). Low panel in Fig. 10 looks like the upper one, except for the density axis. The key is that, now, doping is very low and limits trion generation. Thus, in this case we do not find a significant improvement on the density of photoexcited species.

Fig. 11 shows electron spin relative polarization for the three situations under study, and when photoexciting in resonance with trion level. As expected, curves coincide for cases A and C. By comparing this figure with Figs. 7 and 9, we can note that, in the present case, spin polarization is substantially worse than in the others, being free electron resonant photoexcitation which leads to the best results.

#### IV. SUMMARY AND CONCLUSIONS

First, we should mention here the approximations used in the method of calculation. We assume injection as a tunneling process much shorter than all the other processes involved. Thus, we include doping in the initial conditions as prior to photoexcitation. An important point is the possible effect of the application of external electric fields on trion and electron orientation. We used field strengths less than 10 kV/cm to prevent the possible ionization or diffusion of trion through the structure<sup>3</sup>. Higher external fields can affect spin relaxation times through the Elliott–Yafet mechanism<sup>11</sup>.

The fact that excitonic and trionic electron levels are very close in energy, less than 2 meV in the GaAs<sup>9</sup>, should be reflected in a nonzero trion generation rate when excitons are photoexcited. Thus, a few electrons should be generated in the corresponding state. In the present study the amount of these electrons is negligible because the long pulse leads to a narrow energy dispersion. In this way we have only considered triions formed by means of excitons and free electrons because direct trion generation by resonant exciton photoexcitation can be neglected.

We have used in numerical calculations the eight-coupled Bloch system obtained from the kinetic equation for the one-electron density matrix, projected over the spin states, and taking into account eight possible time-dependent processes.

In summary, we have analyzed the temporal behavior of the density of free electrons, excitons and trions in doped QWs when they are photoexcited with  $\sigma^+$  circularly polarized light. We pay special attention to the electron spin orientation when the sample has different doping concentrations and is subjected to different photoexcitation energy densities. We have considered three cases of resonant photoexcitation corresponding to the three lower conduction electronic levels (free, excitonic and trionic electrons). Also, we have studied the electron spin relative polarization considering the role played by excitons and trions. Our main conclusion is that, for practical purposes, photoexcitation of free electron level leads to a higher spin polarization. Another important point is the relationship between the characteristic photoexcitation density (directly related to the photoexcitation energy density) and doping density. The effect of both variables on the spin polarization is opposite, being significantly more pronounced for the first one. Thus, we have found that increasing photoexcitation enhances spin polarization while this improvement can be achieved by reducing the doping. Our results show a wide variety of responses, caused by the different carrier densities of free and bound electrons and different photoexcitation energy densities. Present results can be checked by means of photoluminescence measures. Photoluminescence experiments of spin density in  $n$ -type GaAs-GaAlAs QWs are available<sup>33</sup>. This work can be applied to any spin relaxation mechanism and other structures by changing the parameters involved. We expect that this work will aid in the design of the experimental conditions to study electron spin dynamics, as well as in stimulating research in this field.

### Appendix A: Coefficients for different processes

Let us check coefficients involved in the mechanisms with which we have been working on: formation ( $F_i$ ), dissociation ( $D_i$ ), and recombination ( $R_i$ ) of excitons and trions. Essentially, we have followed the approach of Berney et al.<sup>37</sup>, specifying as far as possible to our structure and  $T = 5$  K. Thus, we can outline processes as follows:



We first consider the formation coefficients, which depend on carrier and the lattice temperatures,  $T_c$  and  $T$ , respectively. For the exciton coefficient  $C$  we have extrapolated a value of  $2 \times 10^{-12} \text{ cm}^2\text{ps}^{-1}$  from Fig. 1 in the paper of

Berney et al. Considering our coefficient  $F_{exc} = CN_0$ , we obtain a rate of  $F_{exc} \sim 2 \times 10^{-2} \text{ ps}^{-1}$ . In order to estimate bi- and tri-molecular trion formation coefficients we have followed Fig. 2 of the same paper, obtaining  $A_2 \sim 0.6 \times 10^{-12} \text{ cm}^2 \text{ ps}^{-1}$  and  $A_3 \sim 0.2 \times 10^{-22} \text{ cm}^4 \text{ ps}^{-1}$ . Thus, formation rate coefficients we have used for trion formation are  $F_{tr2} = A_2 N_0 \sim 6 \times 10^{-3} \text{ ps}^{-1}$  and  $F_{tr3} = A_3 N_0^2 \sim 2 \times 10^{-3} \text{ ps}^{-1}$ .

Coefficients  $D_i$  have been calculated using the Saha-Eggert equations. In the case that concerns us, Saha-Eggert relations can be written as

$$\begin{aligned} \frac{n_e n_h}{n_{exc}} &= K_{exc}(T) = \frac{m_e m_h}{m_{exc}} \frac{k_B T}{2\pi \hbar^2} \exp\left(-\frac{E_{exc}}{k_B T}\right), \\ \frac{n_e n_{exc}}{n_{tr}} &= K_{tr2}(T) = \frac{m_e m_{exc}}{m_{tr}} \frac{k_B T}{2\pi \hbar^2} \exp\left(-\frac{E_{tr} - E_{exc}}{k_B T}\right), \\ \frac{n_e^2 n_h}{n_{tr}} &= K_{tr3}(T) = \frac{m_e^2 m_h}{m_{tr}} \left(\frac{k_B T}{2\pi \hbar^2}\right)^2 \exp\left(-\frac{E_{tr}}{k_B T}\right), \end{aligned}$$

where  $E_{exc} = 8.60 \text{ meV}$  and  $E_{tr} = 1.33 \text{ meV}$  are the binding energy for exciton and trion, respectively<sup>9</sup>. Here  $m_{exc} = m_e + m_h$ ,  $m_{tr} = 2m_e + m_h$ , where  $m_e$ ,  $m_h$  are the electron and hole effective masses. Thus, we have obtained  $K_{exc} = 8.04 \text{ cm}^{-2}$ ,  $K_{tr2} = 2.04 \times 10^2 \text{ cm}^{-2}$ , and  $K_{tr3} = 7.94 \times 10^{17} \text{ cm}^{-4}$ . Dissociation coefficients will be  $D_{exc} = CK_{exc}$ ,  $D_{tr2} = A_2 K_{tr2}$ , and  $D_{tr3} = A_3 K_{tr3}$ , which numerical values are  $D_{exc} = 1.6 \times 10^{-11} \text{ ps}^{-1}$ ,  $D_{tr2} = 1.2 \times 10^{-10} \text{ ps}^{-1}$ , and  $D_{tr3} = 1.6 \times 10^{-5} \text{ ps}^{-1}$ .

As we can see, the dissociation rates obtained are negligible compared with the formation and recombination rates. Therefore, we have neglected the dissociation coefficients in the system of equations (10-13) because they do not bring any noticeable change in the results.

Let us consider the radiative decay times for excitons and trions, which are the inverse of the recombination coefficients  $R_i$ . As the above coefficients, recombination rates also depend on carrier temperature<sup>4</sup>. Values for our structure and conditions are  $R_{exc} = \tau_{exc}^{-1} = 2.5 \times 10^{-3} \text{ ps}^{-1}$  and  $R_{tr} = \tau_{tr}^{-1} = 4.5 \times 10^{-3} \text{ ps}^{-1}$  for exciton and trion, respectively.

Now, we will consider free electron-hole radiative recombination. Unlike exciton or trion recombination rates, which do not directly depend on their concentrations, free electron recombination does. Free electron must find a free hole to recombine while these charges are already bound in exciton and trion. Following Szczytko et al.<sup>39</sup>, the bimolecular plasma recombination rate will be  $B \sim 10^{-14} \text{ cm}^2 \text{ ps}^{-1}$  and the radiative recombination coefficient of free carriers,  $R_e = BN_0 \sim 10^{-4} \text{ ps}^{-1}$ .



Finally, electron spin relaxation time was taken from Dzhioev et al.<sup>33</sup>, which empirically obtained a value of  $\tau_s = 10$  ns for a structure and conditions similar to ours. About holes, we have used the spin flip time obtained by Schneider et al.<sup>34</sup>, where  $\tau_h = 39$  ps. Thus, the spin relaxation coefficients included in calculations are  $S_e = \tau_s^{-1} = 10^{-4}$  ps<sup>-1</sup> for electrons and  $S_h = \tau_h^{-1} = 2.6 \times 10^{-2}$  ps<sup>-1</sup> for holes.

---

\* Electronic address: paceitun@ull.es

† Electronic address: ajhernan@ull.es

- <sup>1</sup> A. Esser, E. Runge, R. Zimmermann, and W. Langbein, Phys. Rev. B **62**, 8232 (2000); A. Esser, E. Runge, R. Zimmermann, and W. Langbein, Phys. Stat. Sol. (a) **178**, 489 (2000).
- <sup>2</sup> D. Sanvitto, R.A. Hogg, A.J. Shields, D.M. Whittaker, M.Y. Simmons, D.A. Ritchie, and M. Pepper, Phys. Rev. B **62**, R13294 (2000).
- <sup>3</sup> D. Sanvitto, F. Pulizzi, A.J. Shields, P.C.M. Christianen, S.N. Holmes, M.Y. Simmons, D.A. Ritchie, J.C. Maan, and M. Pepper, Science **294**, 837 (2001); F. Pulizzi, D. Sanvitto, P.C.M. Christianen, A.J. Shields, S.N. Holmes, M.Y. Simmons, D.A. Ritchie, M. Pepper, and J.C. Maan, Phys. Rev. B **68**, 205304 (2003).
- <sup>4</sup> M.T. Portella-Oberli, J. Berney, L. Kappei, F. Morier-Genoud, J. Szczytko, and B. Deveaud-Plédran, Phys. Rev. Lett. **102**, 096402 (2009).
- <sup>5</sup> B. Deveaud, L. Kappei, J. Berney, F. Morier-Genoud, M.T. Portella-Oberli, J. Szczytko, C. Piermarocchi, Chem. Physics **318**, 104 (2005).
- <sup>6</sup> M. Hayne, C.L. Jones, R. Bogaerts, C. Riva, A. Usher, F.M. Peeters, F. Herlach, V.V. Moshchalkov, and M. Henini, Phys. Rev. B **59**, 2927 (1999).
- <sup>7</sup> V. Ciulin, P. Kossacki, S. Haacke, J.-D. Ganière, B. Deveaud, A. Esser, M. Kutrowski, and T. Wojtowicz, Phys. Rev. B **62**, R16310 (2000); P. Kossacki, J. Phys.: Condens. Matter **15**, R471–R493 (2003).
- <sup>8</sup> H. Cao, G. Klimovitch, G. Björk, and Y. Yamamoto, Phys. Rev. B **52**, 12184 (1995) and Phys. Rev. Lett. **75**, 1146 (1995).
- <sup>9</sup> P. Aceituno and A. Hernández-Cabrera, J. Appl. Phys. **98**, 013714 (2005).
- <sup>10</sup> D.D. Awschalom and N. Samarth, Physics **2**, 50 (2009); D.D. Awschalom and M.E. Flatté, Nature Phys. **3**, 153 (2007); D.D. Awschalom and N. Samarth, Phys. Today **52**, 33 (1999).
- <sup>11</sup> M.I. Dyakonov (Ed.), *Spin Physics in Semiconductors*, Springer (Berlin, 2008).
- <sup>12</sup> M.W. Wu, J.H. Jiang, and M.Q. Weng, *Spin Dynamics in Semiconductors*, Phys. Reports **493**, 61 (2010).

- <sup>13</sup> G. Finkelstein, V. Umansky, I. Bar-Joseph, V. Ciulin, S. Haacke, J. -D. Ganière, and B. Deveaud, Phys. Rev. B **58**, 12637 (1998); D. Sanvitto, R.A. Hogg, A.J. Shields, M.Y. Simmons, D.A. Ritchie, and M. Pepper, Phys. Stat. Sol. (b) **227**, 297 (2001).
- <sup>14</sup> P. Kossacki, P. Plochocka, B. Piechal, W. Maślana, A. Golnik, J. Cibert, S. Tatarenko, and J. A. Gaj, Phys. Rev. B **72**, 035340 (2005).
- <sup>15</sup> G. Yusa, H. Shtrikman, and I. Bar-Joseph, Phys. Rev. Lett. **87**, 216402 (2001).
- <sup>16</sup> A. Wójs, J.J. Quinn, and P. Hawrylak, Phys. Rev. B **62**, 4630 (2000).
- <sup>17</sup> A. Greulich, R. Oulton, E.A. Zhukov, I.A. Yugova, D.R. Yakovlev, M. Bayer, A. Shabaev, A.L. Efros, I.A. Merkulov, V. Stavarache, D. Reuter, A. Wieck, Phys. Rev. Lett. **96**, 227401 (2006).
- <sup>18</sup> T.A. Kennedy, A. Shabaev, M. Scheibner, A.L. Efros, A.S. Bracker, D. Gammon, Phys. Rev. B **73**, 045307 (2006).
- <sup>19</sup> S. Cortez, O. Krebs, S. Laurent, M. Senes, X. Marie, P. Voisin, R. Ferreira, G. Bastard, J.-M. Gérard, T. Amand, Phys. Rev. Lett. **89**, 207401 (2002).
- <sup>20</sup> S. Laurent, M. Senes, O. Krebs, V.K. Kalevich, B. Urbaszek, X. Marie, T. Amand, P. Voisin, Phys. Rev. B **73**, 235302 (2006).
- <sup>21</sup> W. Ungier and R. Buczko, J. Phys: Condens. Matter **21**, 045902 (2009).
- <sup>22</sup> G.V. Astakhov, M.M. Glazov, D.R. Yakovlev, E.A. Zhukov, W.Ossau, L.W. Molenkamp, and M. Bayer, Semicond. Sci. Technol. **23**, 114001 (2008).
- <sup>23</sup> T. Amand and X. Mari, Chap. 3 in Ref. 11.
- <sup>24</sup> S. Ben-Taboude-Leon and B. Laikhtman, Phys. Rev. B **67**, 235315 (2003).
- <sup>25</sup> I. Žutić, J. Fabian, and S. Das Sarma, Rev. Mod. Phys. **76**, 323 (2004).
- <sup>26</sup> P. Aceituno and A. Hernández-Cabrera, Phys. Rev. B **78**, 115308 (2008).
- <sup>27</sup> O. E. Raichev, Phys. Rev. B **51**, 17713 (1995); A. Hernández-Cabrera and P. Aceituno, Phys. Rev. B **61**, 15873 (2000).
- <sup>28</sup> F.T. Vasko and O.E. Raichev, *Quantum Kinetic Theory and Applications: Electrons, Photons, Phonons*, Springer (New York, 2005).
- <sup>29</sup> Y. Ohno, R. Terauchi, T. Adachi, F. Matsukura, and H. Ohno, Physica E **6**, 817 (2000).
- <sup>30</sup> W.J.H. Leyland, G.H. John, R.T. Harley, M.M. Glazov, E.L. Ivchenko, D.A. Ritchie, I. Farrer, A.J. Shields, M. Henini, Phys. Rev. B **75**, 165309 (2007).
- <sup>31</sup> A. Vinattieri, J. Shah, T. C. Damen, D. S. Kim, L. N. Pfeiffer, M. Z. Maialle and L. J. Sham, Phys. Rev. B **50**, 10868 (1994).
- <sup>32</sup> N. J. Harmon, W. O. Putikka, and R. Joynt, Phys. Rev. B **81**, 085320 (2010).

- <sup>33</sup> R. I. Dzhioev, V. L. Korenev, M.V. Lazarev, V. F. Sapega, D. Gammon and A. S. Bracker, *Phys. Rev. B* **75** 033317 (2007).
- <sup>34</sup> P. Schneider, J. Kainz, S. D. Ganichev, S. N. Danilov, U. Rössler, W. Wegscheider, D. Weiss, W. Prettl, V. V. Bel'kov, M. M. Glazov, L. E. Golub, and D. Schuh, *J. Appl. Phys.* **96**, 420 (2004).
- <sup>35</sup> B. Baylac, T. Amand, X. Marie, B. Dareys, M. Brousseau, G. Bacquet, V. Thierry-Mieg, *Solid State Commun.* **93**, 57 (1995).
- <sup>36</sup> Ph. Roussignol, P. Rolland, R. Ferreira, C. Delalande, G. Bastard, A. Vinattieri, J. Martínez-Pastor, L. Carraresi, M. Colocci, J.F. Palmier, and B. Etienne, *Phys. Rev. B* **46**, 7292 (1992).
- <sup>37</sup> J. Berney, M.T. Portella-Oberli, and B. Deveaud-Plédran, arXiv:0901.3645 [cond-mat.mtrl-sci] (2009).
- <sup>38</sup> H. Hoffmann, G.V. Astakhov, T. Kiessling, W. Ossau, G. Karczewski, T. Wojtowicz, J. Kossut, and L.W. Molenkamp, *Phys. Rev. B* **74**, 073407 (2006).
- <sup>39</sup> J. Szczytko, L. Kappei, J. Berney, F. Morier-Genoud, M.T. Portella-Oberli, and B. Deveaud, *Phys. Rev. Lett.* **93**, 137401 (2004).

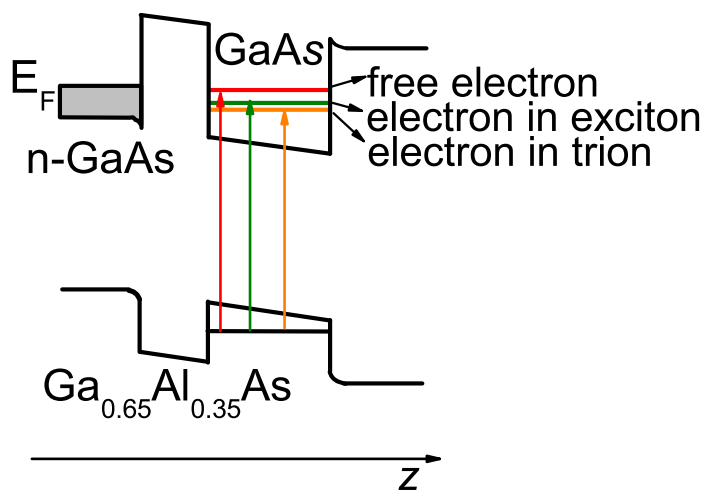


FIG. 1: (Color online) Scheme of the doped quantum well under study.

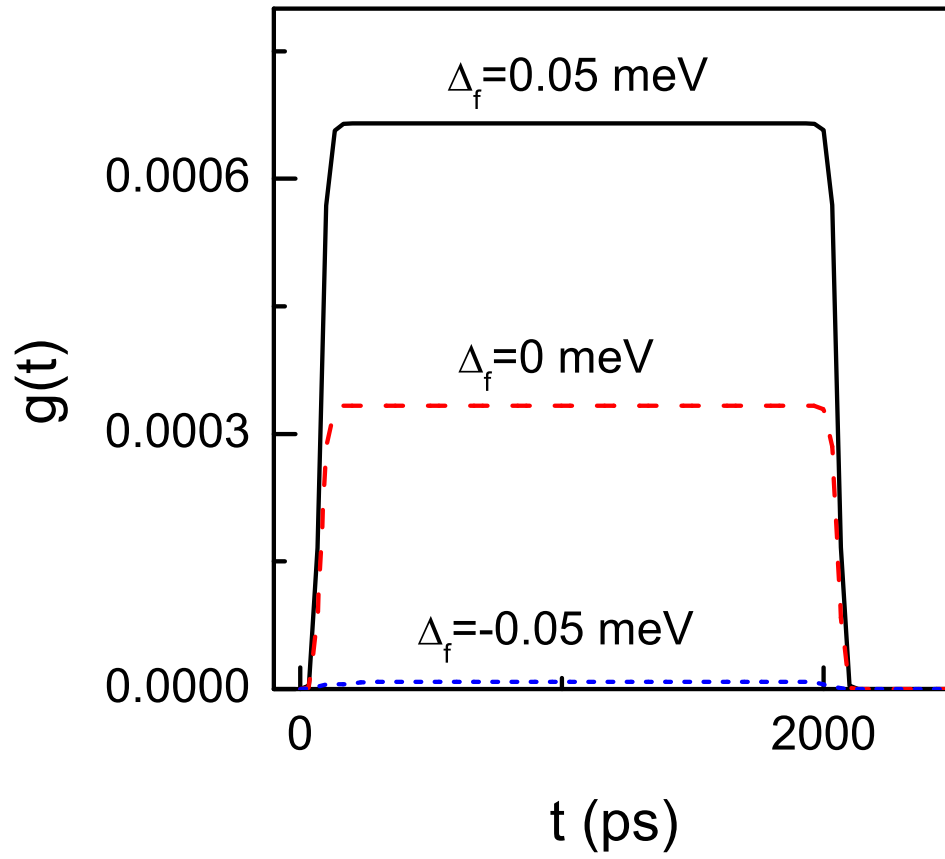


FIG. 2: (Color online) Generation function for  $\tau_p = 2000$  ps and  $\tau_f = 10$  ps. Solid line:  $\Delta = 0.05$  meV. Dashed:  $\Delta = 0$  meV. Dotted:  $\Delta = -0.05$  meV.

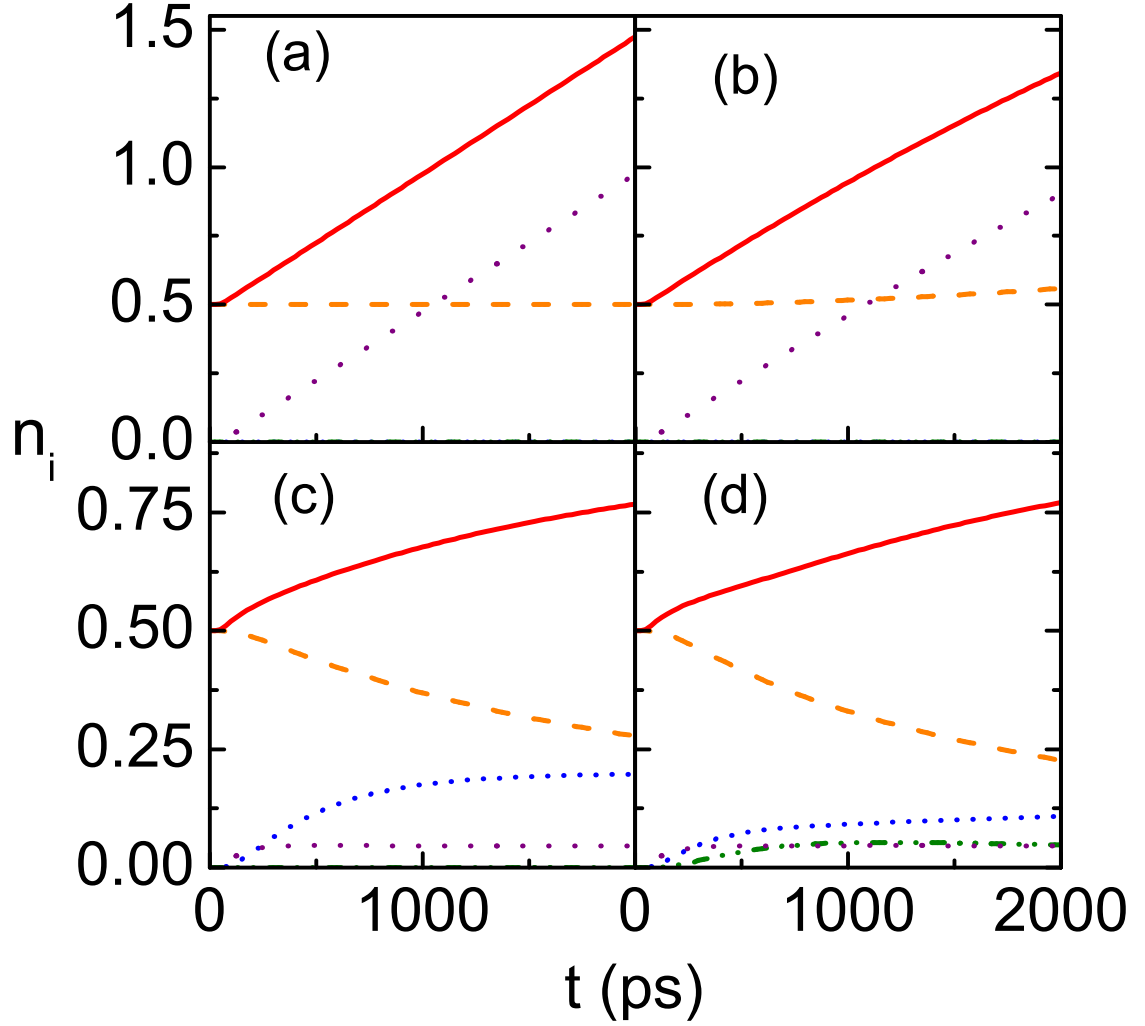


FIG. 3: (Color online) Normalized density versus time for free electron resonant photoexcitation. Considering only doping and photoexcitation (a), adding recombination electron-hole and spin-flip (b), considering also formation and recombination of excitons (c), and including the presence of trions (d). Solid line (red): spin-down free electrons; dashed line (orange): spin-up free electrons; dash-dot-dotted line (purple): up and down free holes; short-dashed line (blue): excitons; and dash-dotted line (green): trions.

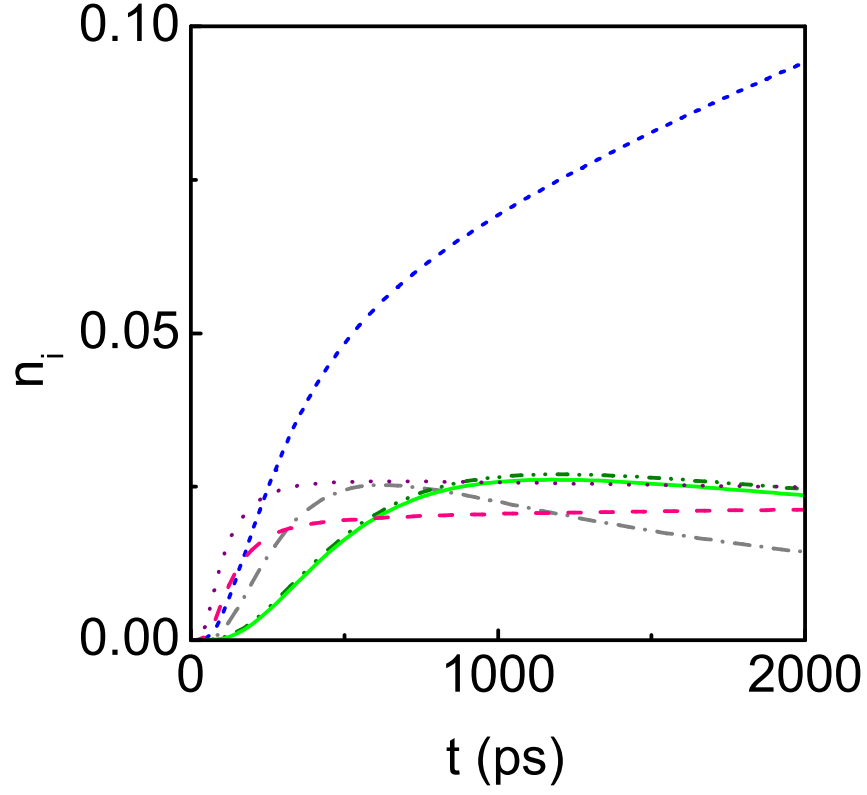


FIG. 4: (Color online) Normalized density versus time. The same as in Fig 3d but amplifying the region for excitons, trions and holes. Short-dashed line (blue): excitons  $\uparrow\downarrow$ ; dash-dotted line (grey): excitons  $\downarrow\uparrow$ ; dash-dot-dotted line (green): trions  $\uparrow$ ; solid line (light green): trions  $\downarrow$ ; dotted line (purple): holes  $\uparrow$ ; and dashed line (pink) holes  $\downarrow$ .

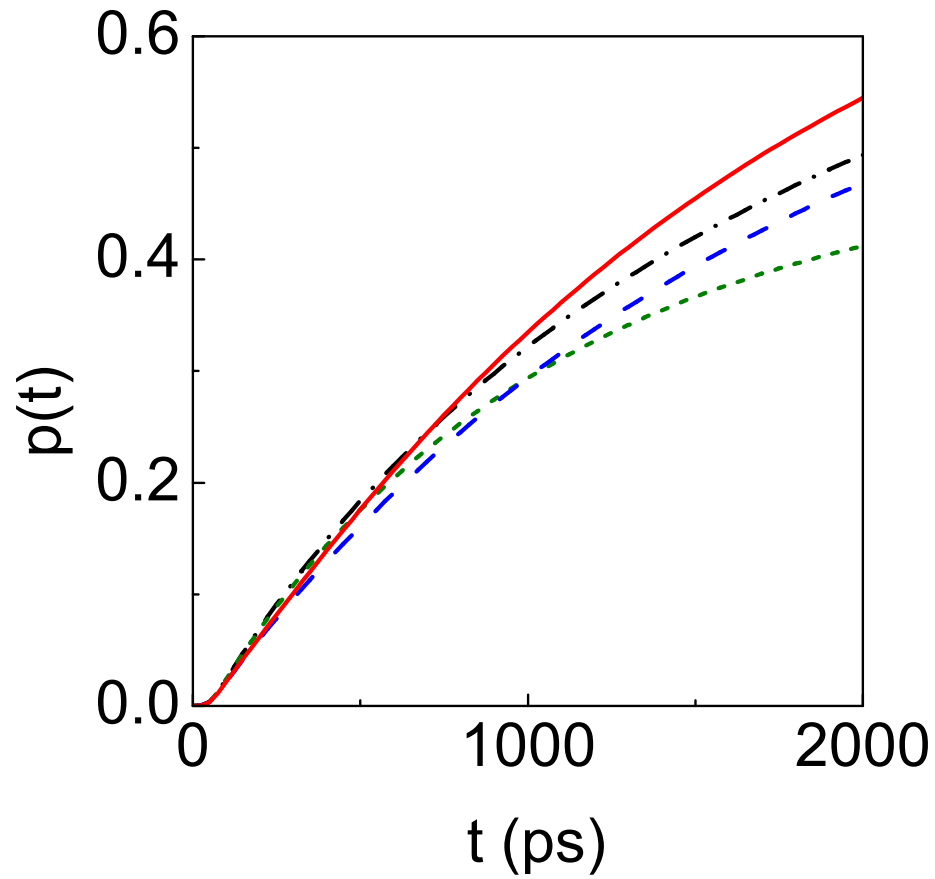


FIG. 5: (Color online) Polarization versus time. Considering only doping and photoexcitation (dash-dotted black line), adding recombination electron-hole and spin-flip (dotted green line), considering also formation and recombination of excitons (dashed blue line), and including the formation of trions (solid red line).



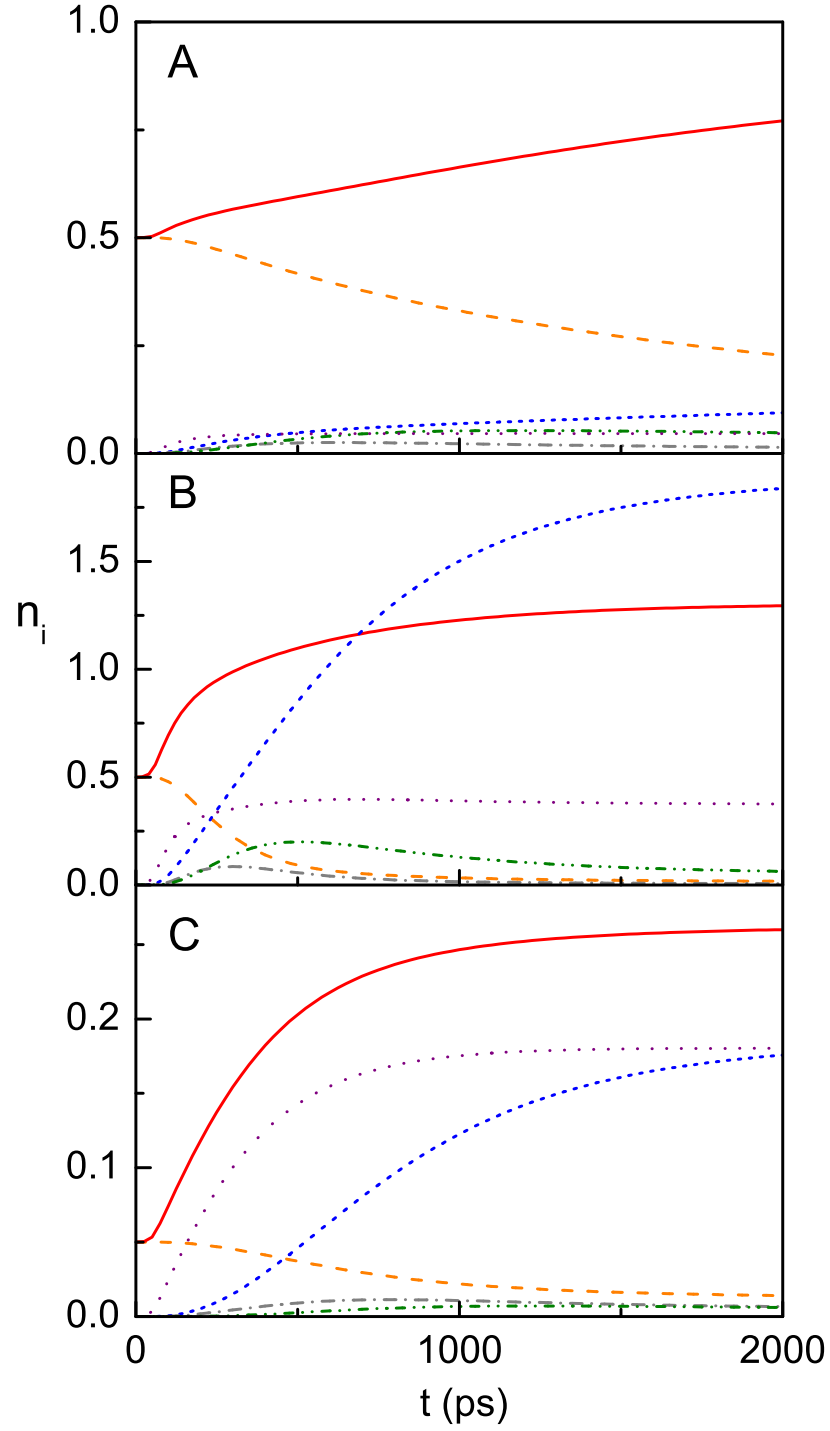


FIG. 6: (Color online) Normalized density time evolution for free electron resonant photoexcitation. Upper panel: case (A),  $N_{ph} = N_D = N_0$ ; middle panel: case (B),  $N_{ph} = 10N_0$ ,  $N_D = N_0$ ; and lower panel: case (C),  $N_{ph} = N_0$ ,  $N_D = N_0/10$ . Colors and lines as in Figs. 3 and 4.

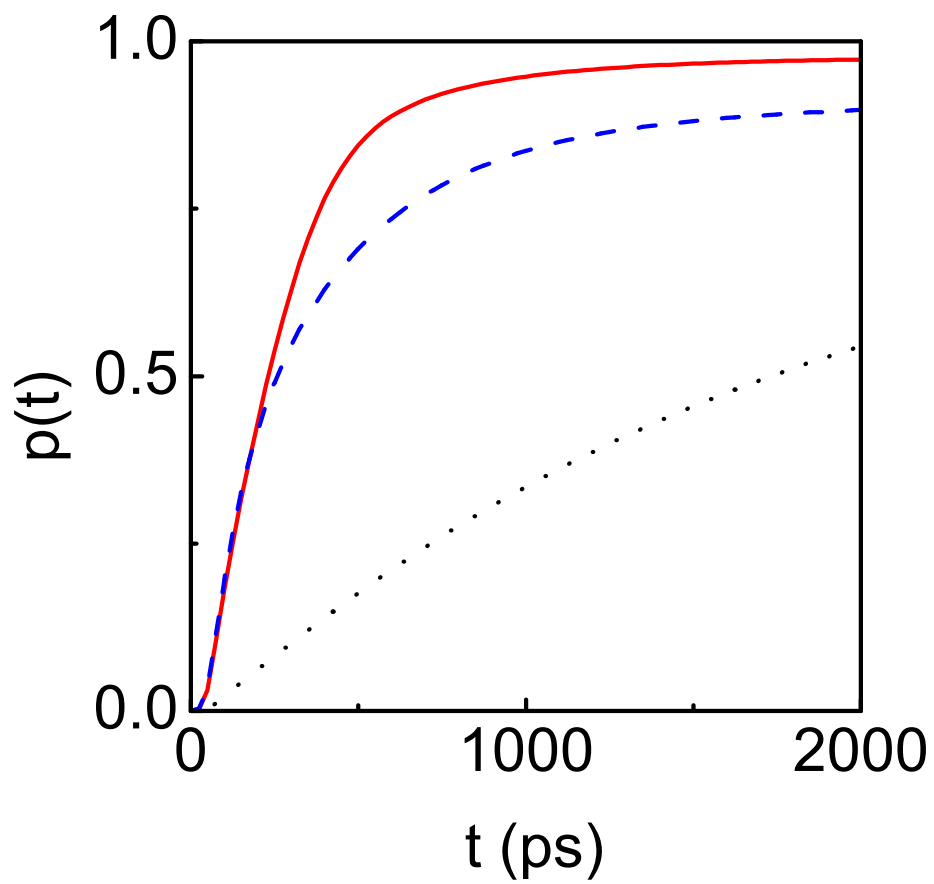


FIG. 7: (Color online) Relative polarization versus time. Case (A): dotted (black) line; case (B): solid (red) line; and case (C): dashed line (blue).

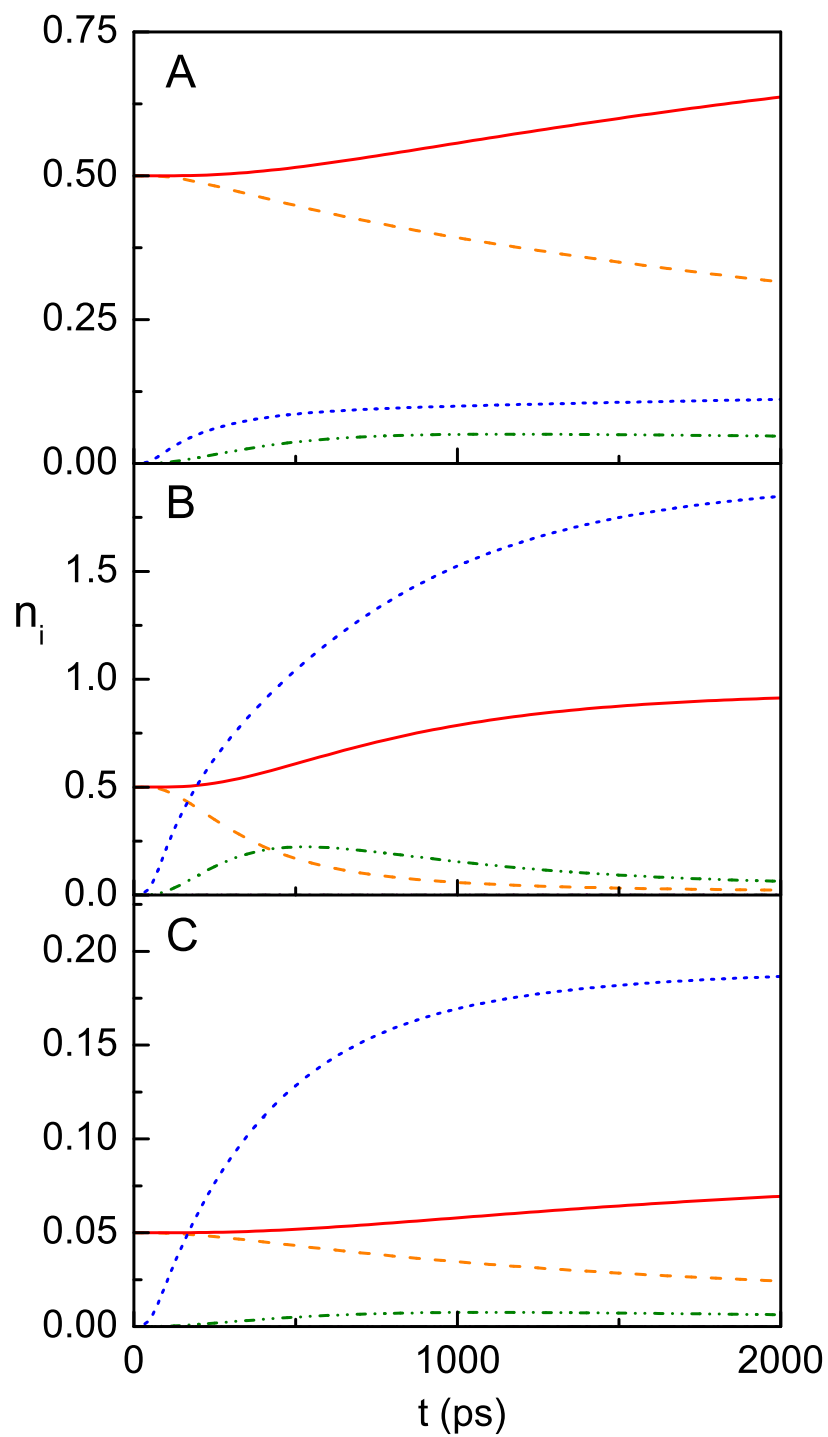


FIG. 8: (Color online) Normalized density versus time for exciton level resonant photoexcitation. Upper, middle and lower panels correspond to the same cases as in Fig. 6, with the same meaning for colors and lines.

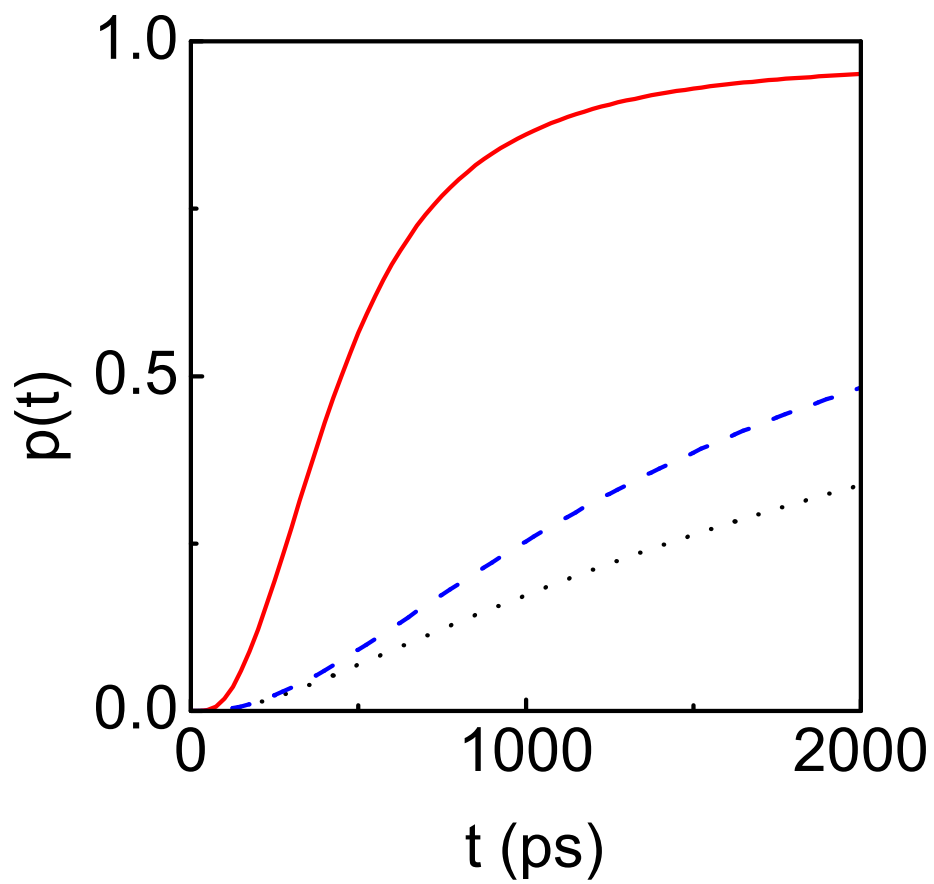


FIG. 9: (Color online) Electron spin polarization versus time for exciton resonant photoexcitation. Colors and lines as in Fig 7.

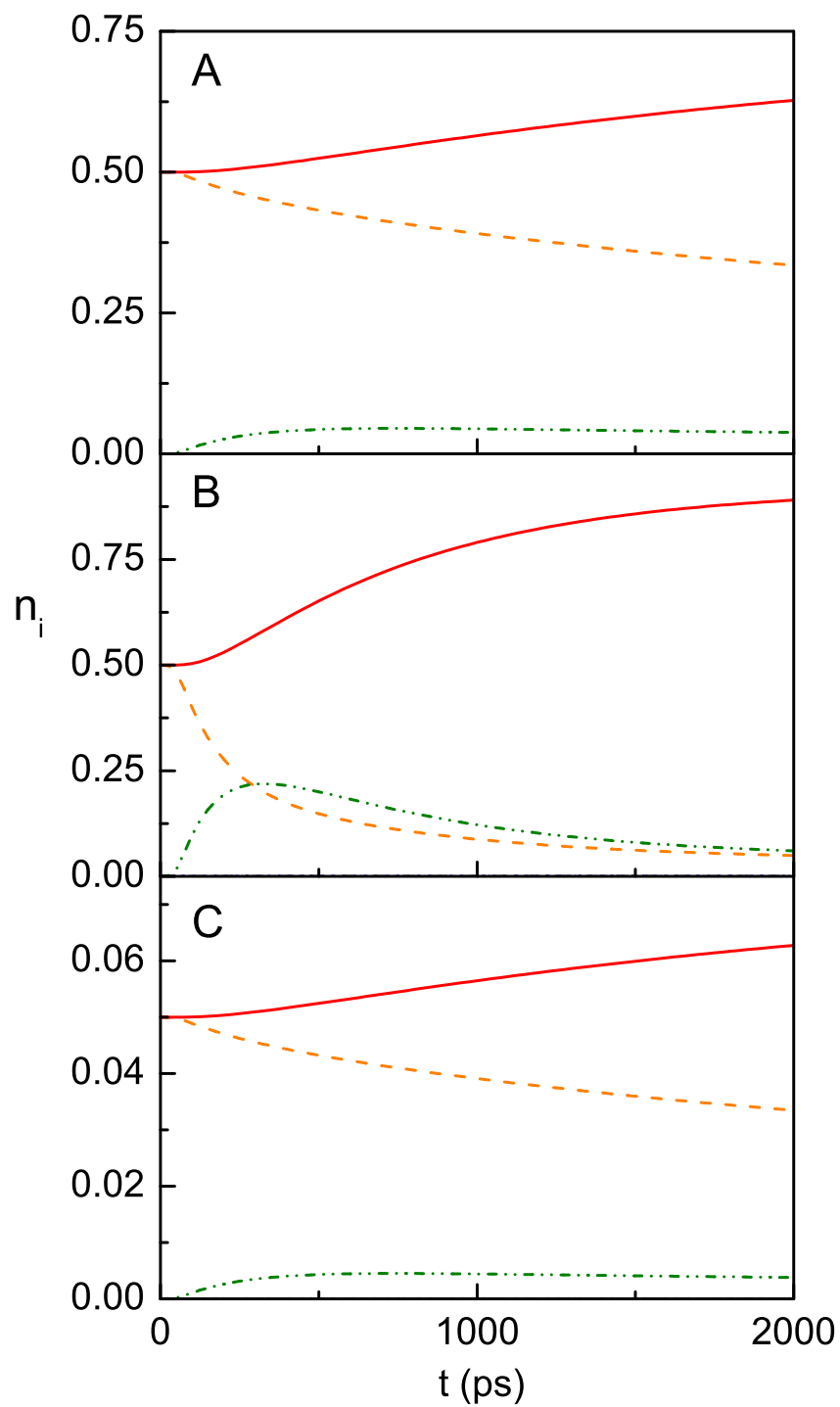


FIG. 10: (Color online) Relative density versus time for trion level resonant photoexcitation. Upper, middle and lower panels for the same cases as Fig. 6, with the same meaning for colors and lines.

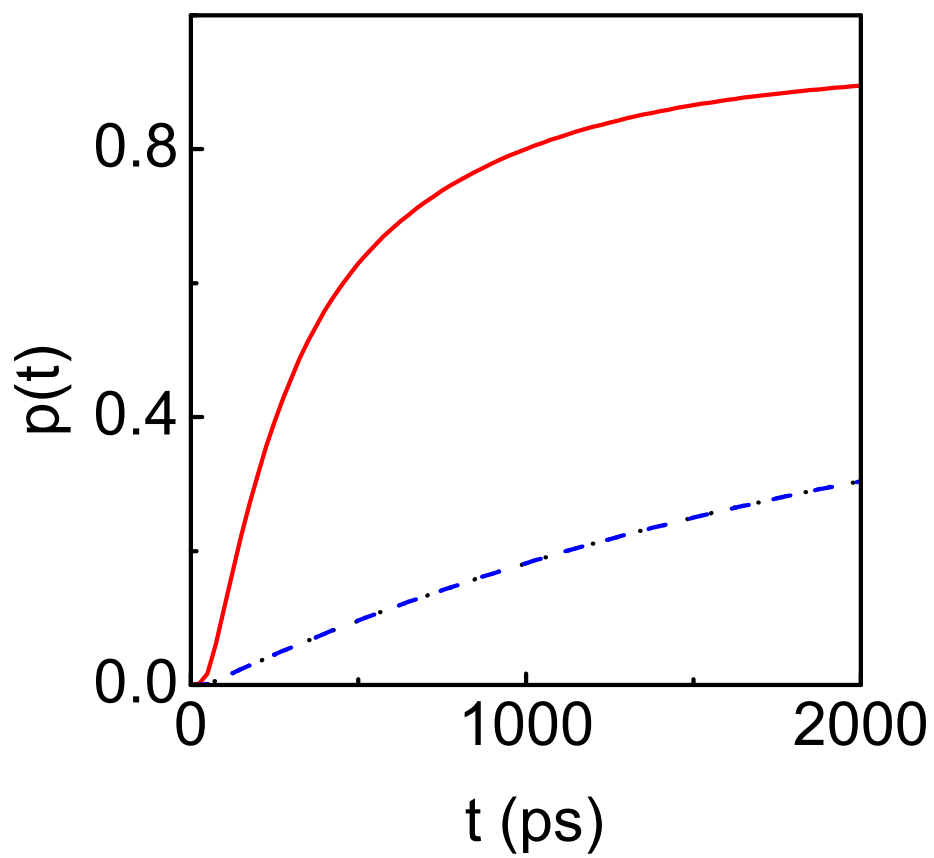


FIG. 11: (Color online) Electron spin polarization versus time for trion resonant photoexcitation. Colors and lines as in Fig 7.